DOI: 10.12442/j.issn.1002-185X.20240154

Preparation and brazing performance study of nickel coated Al_2O_3 reinforced low silver SnAgCu composite solder

Bingying Wang 1,2, Keke Zhang 1, yuchun Fan1,Jina Wu1, Limeng Guo2, Huigai Wang 1, Nannan Wang1

1Henan University of Science and Technology, Luoyang 471000, China; 2Luoyang Institute of Science and Technology, Luoyang,471023, China

ABSTRACT: Dopamine polymerization reaction and hydrothermal method was used to prepare nickel coated alumina reinforcement phase; Preparation of nickel coated alumina (Ni/Al_2O_3) reinforced Sn1.0Ag0.5Cu (SAC105) composite material alloy using traditional casting method; The result showed that the nickel coating layer was continuous but with uneven thickness.The interface between nickel and aluminum oxide was a metallurgical bonding coherent interface relationship; The strength, toughness, and wettability of the SAC105 solder with the substrate have been improved, while the conductivity has not decreased significantly. The optimal doping amount was determined by comprehensive analysis when the doping amount of the reinforcing phase was 0.3wt%. The fracture mode of composite material alloy has shifted from a mixed mode of toughness and brittleness to a pure toughness fracture mode composed only of a large number of dimples.The prepared composite brazing material was made into solder paste for copper plate lap joint experiments. The maximum shear strength was achieved when the doping amount was 0.3wt% The growth index of IMC at the brazing interface of Ni/Al_2O_3 reinforced Sn1.0Ag0.5Cu composite brazing material was linearly fitted to n=0.39, which can be used to determine the joint effect of grain boundary diffusion and bulk diffusion on the growth of IMC at the interface.

Keywords: Composite solder; Enhanced phase; Aggregation method; Hydrothermal method; interface.

Due to the harmful effects of lead on the environment, Scholars are increasingly paying attention to the research and development of lead-free materials[1, 2]. However, SnAgCu solder with high silver content has certain drawbacks, such as poor drop impact performance and high cost[3-5]. Therefore, the study of low silver alloy solder has become a research direction for many scholars.Previous studies have found that low silver content can lead to some issues with the material. For example, the spreading area of the material decreases and the strength is lower during the tensile process[6, 7]. Therefore, how to develop a low silver solder with superior comprehensive performance has become a focus of attention for many scholars .

There are currently two common methods to improve composite solder: one is to add some alloy elements to the solder for melting. Another method is to add a certain amount of second phase to the original solder [8-10]. In recent years, the doping of inert particles has become one of the research hotspots in the doping of second phase particles[11-13]. Nano alumina has the advantages of light weight and low price, meeting the requirements of high-density packaging technology [14, 15].However, the interface adhesion between nano alumina and the solder alloy matrix is weak, resulting in poor wettability and toughness of the composite solder[16-19]. Nickel particles have advantages such as larger specific surface area, uniform dispersion of active components, and difficulty in sintering, which can effectively prevent agglomeration. There are reports that moderate amounts of nickel can improve the microstructure and service performance of solder alloys [20].

Due to the poor wettability of ceramics and metals, it is difficult to connect them together. Unlike metal bonds, ceramics are composed of covalent bonds.[21] Therefore, the bonding strength of the ceramic metal interface is also poor. Dopamine polymerization reaction was adopted, Firstly, amorphous carbon film was applied as a transition layer on the surface of alumina, as it is more capable of adsorbing nickel ions. Then, nickel nitrate was used as the precursor by hydrothermal method, and after the reaction was completed, the amorphous carbon film was burned off and the nickel coated layer was left behind by calcination in an air atmosphere.

1 Experiment

The Sn1.0Ag0.5Cu power used in the experiment was provided by Changsha Tianjiu Company with a particle size of 300 mesh. Dopamine hydrochloride and trimethylaminomethane were purchased from McLean Technology Co. Ltd. (China). Nickel nitrate hexahydrate (AR) and nano- Al_2O_3 particles were purchased from PanTian Co. Ltd. (Shanghai, China)

The reinforcing phase of the composite solder used in this experiment was Al_2O_3coated nickel, and the reaction principle of its coating was shown in Fig.1.The specific description

Foundation item: National Natural Science Foundation of China (U1604132); Central Plains Talents Program - Fund of Central Plains Leading Talents (ZYYCYU002130);Key Technology Research and Development Program of Henan Province (222102230114); Major Scientific Research Foundation of Higher Education of Henan Province (23B430003)

Corresponding author:Keke Zhang,Ph.D.,Professor,School of Materials Science and Engineering,Henan University of Science and Technology ,Luoyang 471023,P.R.China,E-mail:zhkeke@haust.edu.cn

Rare Metal Materials and Engineering

was as follows:a certain amount of Al_2O_3 nanoparticles and dopamine were dispersed into a tri (hydroxymethyl) aminomethane buffer solution.Dopamine underwent spontaneous oxidative forming polydopamine coated Al_2O_3partiles.Then, after heat treatment in an argon atmosphere, polydopamine was converted into nitrogen-containing carbon and coated on the surface of Al_2O_3. Then, the nickel salt was heated and decomposed using hydrothermal method, and the carbon coated in the first step was burned off in an air atmosphere. Finally, the nickel layer was coated on the surface of Al_2O_3.

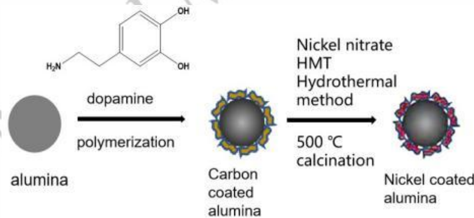

Fig.1 Principle diagram of Al_2O_3 coated nickel reaction

The equation for hydrothermal reaction are as follows:

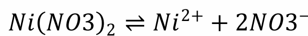

$$Ni(NO3)_2 \rightleftharpoons Ni^{2+} + 2NO3^{-}$$

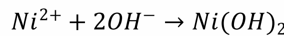

$$Ni^{2+} + 2OH^{-} \rightarrow Ni(OH)_2$$

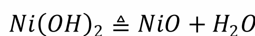

$$Ni(OH)_2 \triangleq NiO + H_2O$$

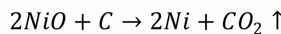

$$2NiO + C \rightarrow 2Ni + CO_2 \uparrow$$

The preparation of brazed joints in this experiment was carried out using copper plate overlap method. Composite solder paste is used to fill the gap between two copper plates. Sn1.0Ag0.5Cu alloy powder, with an average size of approximately 25-40 μm. Nano Ni/Al_2O_3 particles with an average size of 200nm were used to synthesize the composite solder Sn1.0Ag0.5Cu-x (Ni/Al_2O_3) x=0, 0.1, 0.3, 0.5wt%).The specific process is as follows: Ni/Al_2O_3 particles and different weights of paste were weighed using an electronic balance, manually mixed, and quickly stirred for 30 minutes. Afterwards, add Sn1.0Ag0.5Cu alloy powder to the mixture and manually maintain stirring for at least 30 minutes to ensure that the composite solder with a certain viscosity and Ni/Al_2O_3 particles are uniformly dispersed in the composite solder [22].The specific size of copper plate overlap is shown in Fig. 2.

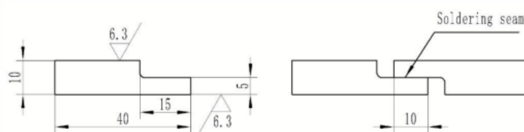

Fig. 2 Schematic diagram of copper plate overlap during brazing process

The morphology of the prepared Ni-Al2O3 was observed by scanning electron microscope (SEM) and transmission electron microscope (TEM). The phase structure was analyzed by X-ray diffractometer (XRD, accelerating voltage 40 kV, scan range 20-90) with Cu Karadiation at a scan rate of 4 Å/min. The composition of Ni-Al_2O_3 was measured by SEM attached energy dispersive spectroscopy (EDS).The polished specimens were etched in a mixture of methanol and hydrochloric acid (92 vol% methanol and 8 vol% hydrochloric acid) for 20 s. The morphology of the prepared samples and the morphology of the IMC layer were shaped by SEM and energy dispersive spectroscopy (EDS).

2 Results and discussion

2.1 Composition and morphology analysis of nickel coated Al_2O_3

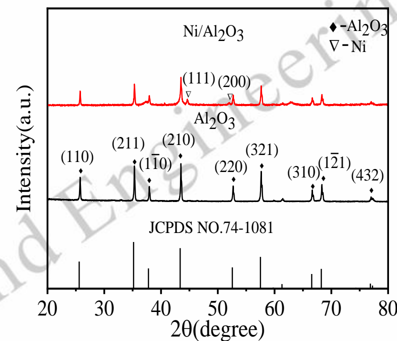

Fig.3 XRD analysis of Al_2O_3 before and after nickel coated

Fig. 3 shows the XRD phase structure analysis of Al_2O_3 before and after nickel coated. From the graph, it can be seen that sharp characteristic peaks were displayed at 25.6 °, 35.2 °, 37.8 °, 43.4 °, 52.6 °, 57.5 °, and 66.5 °, corresponding to the (110), (211), (1-10), (210), (220), (321), (310), and (1-21) planes of the Al_2O_3 crystal structure, respectively. Its peak value is consistent with the standard card (PDF # 74-1081). The peaks of nickel appear at 44.5 °and 51.8 °, corresponding to the (111) and (200) crystal planes, respectively.

Rare Metal Materials and Engineering

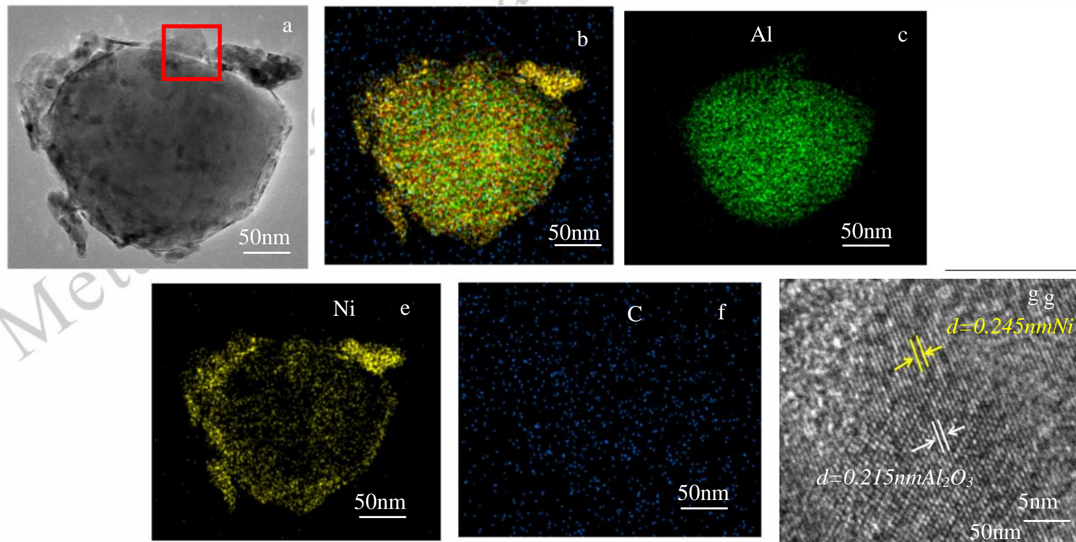

Fig.4 TEM analysis of Al_2O_3 after nickel coated (a)TEM image; (b)EDS mappings of their overlay; (c) Al; (d) O; (e) Ni; (f)C；(g) High Resolution Analysis of Region 1 in Fig.（a）

Fig.4 shows the TEM analysis of nickel coated Al_2O_3. From Fig. 4(e),the distribution of Ni elements was uniform and continuous.The elemental distribution diagrams of Al,O,C are shown in Fig.4 (c), (d), (f),respectively. From the Fig.4(f), it can be seen that the distribution points of element C are very scattered, without obvious bright areas. This indicated that the amorphous carbon in the early stage had already been decomposed.Fig. 4(g) shows the HRTEM images of the interfaces. The Ni/Al_2O_3 interface can be assigned to Ni (111)/ Al_2O_3(110) interface, where $d_{Ni(111)}$=0.245nm and d_{Al2O3}(110)=0.215nm

According to the mismatch (1)

$$\varepsilon=(d_\alpha-d_\beta)/d_\alpha \quad (1)$$

ε is the mismatch between the two interfaces, dα is the interplanar spacing of interface α (nm), dβ is the interplanar spacing of interface β, (nm). According to the formula, ε=0.13 is calculated. According to the literature [23],If e ranges from 0.05 to 0.25, and the interface shows a semi-coherent relationship.This means that the interface is metallurgical bonding .SoThe coating film usually doesn't fall off.

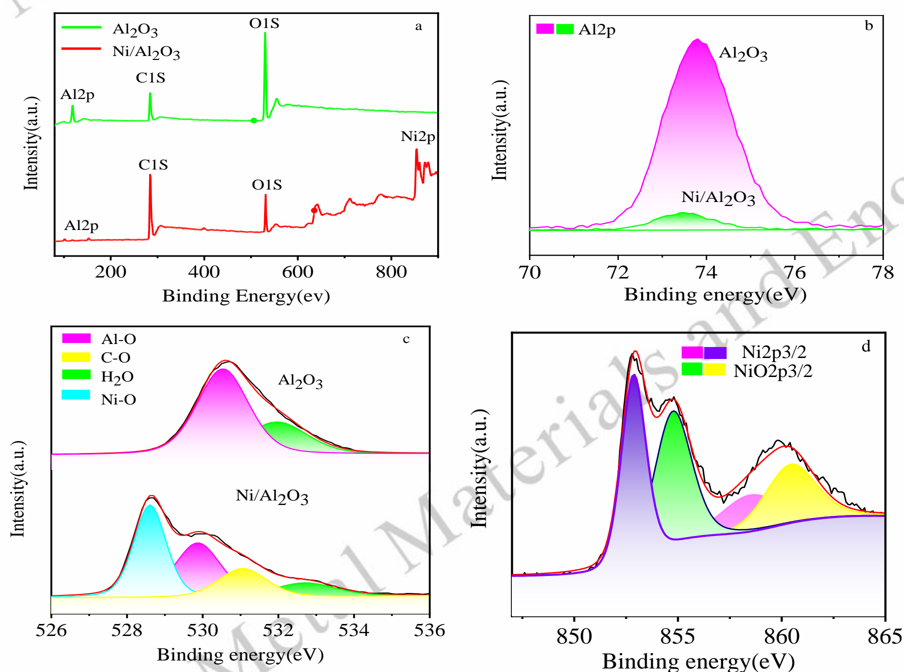

Rare Metal Materials and Engineering

Fig.5 xps spectrum of Al_2O_3 and modified-Al_2O_3 (a)Total spectrum;(b)Al 2p;(c)O1s;(d)Ni2p

XPS is a common surface analysis method that obtains information on the composition, chemical state, and molecular structure of Al,Ni, and O elements on the sample surface from the peak positions and shapes of the XPS spectrum. The experimental results are shown in Fig.5. Fig.5 (a) shows the peak of total characteristic spectrum lines of alumina before and after nickel modification, As shown in the figure, there were more characteristic peaks of nickel in the modified spectrum. Due to nickel coating, the peak aluminum content on the surface was significantly reduced. Fig.5 (b) shows the spectrum of aluminum before and after nickel modification. It can be seen that the peak appears around 74ev, which was determined by literature to be Al2p[24]. The decrease in peak intensity was consistent with the results of the total spectrum, which was due to the reduction of surface aluminum elements caused by nickel coating. Aluminum oxide did not participate in the reaction[25].Fig.5 (c) shows the O1s peak before and after nickel modification.According to the NIST XPS database, The nickel coated alumina sample increased C-O and Ni-O at the peak values of 531.2eV and 528.3eV, respectively. Fig. 5 (d) shows the Ni1s peak in the nickel coated Al_2O_3 sample. Peaks of Ni2p3/2, NiO2p3/2 (sat), Ni2p3/2 and NiO2p3/2 (sat) were detected at positions 852.9eV, 854.8eV, 858.6eV, and 860.5eV, respectively.These results indicated the presence of nickel in the sample, which was consistent with the previous XRD analysis results.

2.2 The microstructure and properties of composite solder.

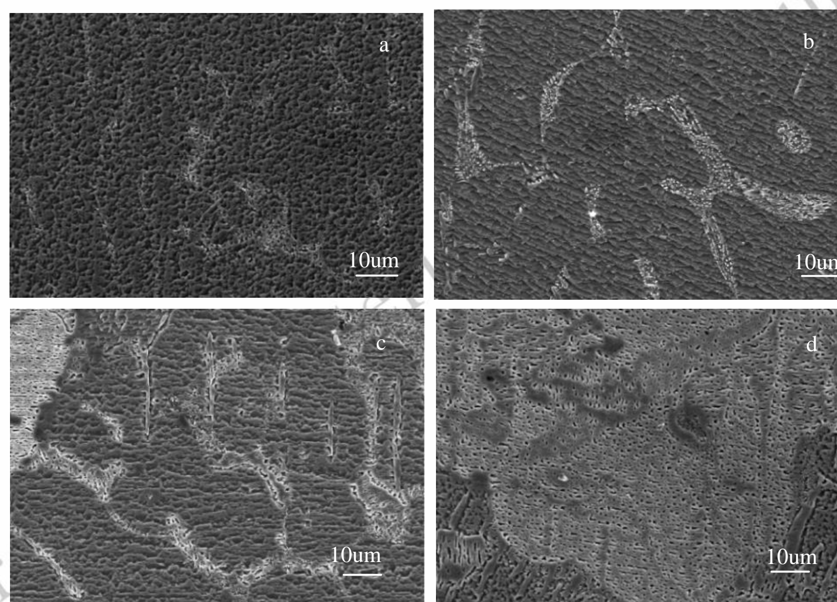

Fig.6 Microstructure of Composite Solder(SAC105-x Ni/Al_2O_3) (a)Raw solde;(b)x=0.1wt%; (c)x=0.3wt%; (d)x=0.5wt%

Fig.6 shows the microstructure of the composite brazing material. From Fig. 6 (a), it can be observed that the microstructure of SAC105 matrix brazing material mainly included β-Sn and eutectic structure.The gray block organization area was β-Sn, the eutectic structure was a white area,which mainly concentrated on the grain boundary structure line. With the increase of Ni/Al_2O_3 particles addition, the composite solder of β-Sn tissue area gradually decreased, and the proportion of eutectic tissue gradually increased.The possible reason for this may be that most of the Ni/Al_2O_3 particles adhere to the surface of the solder alloy powder, leading to an increase in the surface diffusion resistance of atoms during the sintering process.Due to the merging and growth of β-Sn grains were limited, the average size of β-Sn grains decreased and the proportion of eutectic structure increased.When the amount added Ni/Al_2O_3 particles exceeded 0.5wt.%,agglomeration occured,which reduced its uniformity in the solder matrix. This further weakened the grain refinement effect and led to coarsening of the eutectic structure[26].

Rare Metal Materials and Engineering

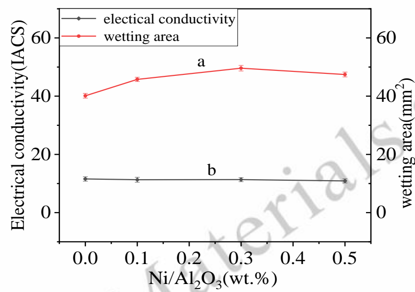

Fig.7 Performance of SAC105 solder reinforced with different mass fractions of Ni/Al_2O_3(a) Wetting area; (b) Conductivity

The curve (a) in Figure 7 shows the trend of wetting area of composite solder with different mass fractions of Ni/Al_2O_3 reinforcement phases.Wettability represents the degree of diffusion of fluid on solid surfaces[27].As the mass fraction of Ni/Al_2O_3 in the solder matrix increased, the wetting area value first increased and then decreased. The reason for this change in wettability may be explained as follows:During the wetting process,Ni/Al_2O_3 particles filled the interface between the composite solder and the copper substrate with brazed joints through capillary action[28].When Ni/Al_2O_3 particles were added, the agglomeration of Ni/Al_2O_3 in the solder matrix increased, which reduced the gap in the interface IMC layer, leading to thermal expansion between the solder matrix and reinforcement phase, and also causing oxidation of the composite solder, thereby reducing its fluidity and wettability [29-31]. The curve (b) in Fig. 7 shows the trend of electrical conductivity of Ni/Al_2O_3 reinforced phase alloy with different mass fractions. As the mass fraction of Ni/Al_2O_3 increased, the electrical conductivity of the composite solder slightly decreased. This change can be explained by Mattison's law: the electrical resistivity of metal materials can be expressed as:: $\rho = \rho(T) + \rho(0)$ is a temperature dependent resistivity $\rho(T)$ and it is called the basic resistance.is related to impurity concentration, point defectsand $\rho(0)$ and it is called solute (impurity) resistance of metals[32]. Introducing Ni/Al_2O_3 into the SAC105 solder matrix results in defects such as vacancies, dislocations, and interfaces, which hinder electron migration and increase resistance. However, due to the small amount of reinforcing phase added, the decrease in conductivity is not significant.

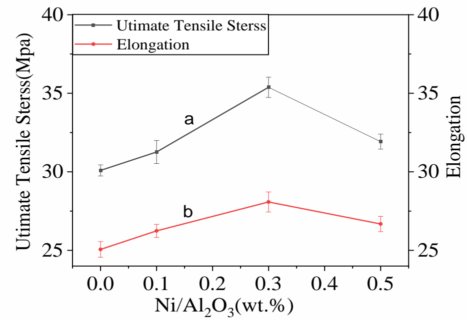

Fig.8 illustrates the mechanical properties of SAC105 solder reinforced with different mass fractions of Ni/Al_2O_3. As shown in the figure, with the increase of the doping mass ratio of the reinforcing phase, both the tensile strength and elongation show the same trend of first increasing and then decreasing. When the doping mass fraction reaches 0.3%, the tensile strength and elongation of the modified solder reach the maximum, which were 16% and 8% higher than that of the original solder, respectively. Afterwards, as the mass fraction of the enhanced phase doping continued to increase to 0.5%, the tensile strength and elongation of the brazing material decreased to 32MPa and 26%, respectively.The reason for the decrease in strength and elongation energy may be due to excessive agglomeration of reinforcing phases.In summary, when 0.3% Ni/Al_2O_3 was added, the tensile strength and elongation (35.3MPa and 28.1%) of the composite solder reach their respective maximum values, which is better than other similar nanomaterials previously reported to enhance Sn1.0Ag0.5Cu composite solder [33]. Meanwhile, compared to commercial Sn3.0Ag0.5Cu[34, 35], the UTS results are basically the same, with higher elongation than commercial Sn3.0Ag0.5Cu. These results indicate that a new type of lead-free solder can obtain materials with high strength and ductility.

2.3 Shear strength and interface IMC structure of brazed joints

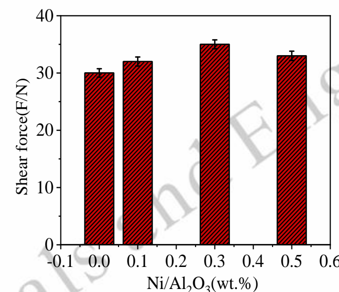

Fig.9 Shear strength of solder joint with SAC105-xNi/Al_2O_3 solders (x=0,0.1wt%.0.3wt%.0.5wt%)

Fig.9 illustrates the shear strength of solder joints brazed with different Ni/Al_2O_3 contents. From the bar chart, it can be seen that as the content of Ni/Al_2O_3 increased by 0.1%, 0.3%, and 0.5% respectively, the shear strength of the composite

Rare Metal Materials and Engineering

alloy increased by 6%, 16%, and 10% compared to the original Sn1.0 Ag0.5Cu solder.

Fig.8 Mechanical properties of SAC105 solder reinforced withdifferent mass fractions of Ni/Al_2O_3

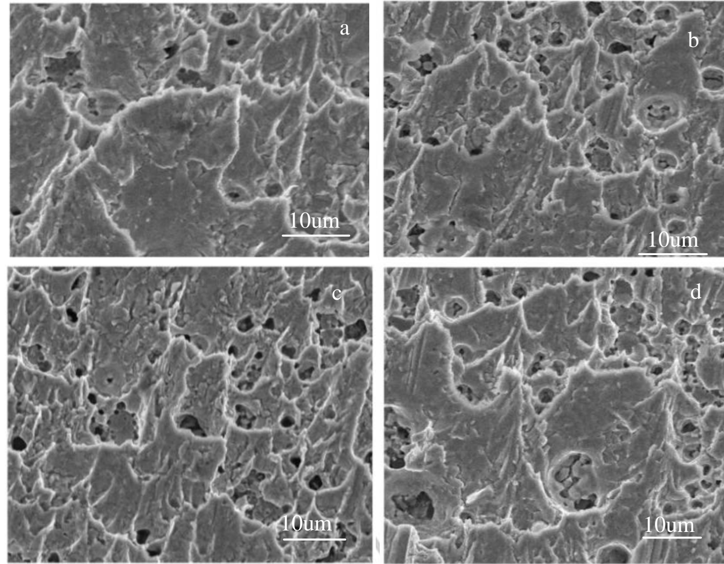

Fig.10 Microstructure of SAC105-xNi/Al_2O_3 (a)Raw solder; (b)x=0.1wt%;(c)x=0.3wt%;(d)x=0.5wt%

Fig.10 illustrates the fracture morphology of SAC105 solder with different reinforcement phase contents. The fracture morphology of the solder substrate is shown in Fig.10 (a). The fracture surface was mainly composed of ductile dimples and brittle cleavage planes, indicating that its fracture mode was ductile brittle fracture.With the increase of Ni/Al_2O_3 content, the number and depth of ductile dimples increased, indicating a greater degree of plastic deformation. In addition, the number of cleavage planes on the fracture surface decreased. As shown in Fig. 10 (c), when the doping mass fraction reached 0.3%, the number of dimples was the highest and the plasticity was the best, which was consistent with the previous change in elongation.

Based on the above analysis, it can be concluded that the optimal addition amount was 0.3%. At different brazing times, brazing experiments were conducted on composite solder with 0.3% enhanced phase, and the diffusion mechanism of IMC layer formation in brazed joints was studied.

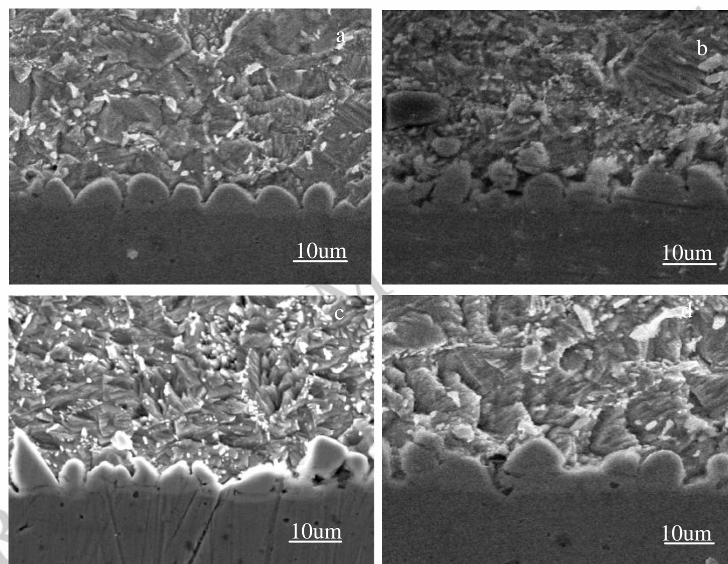

Fig. 11 Morphology of IMC at the joint interface of SAC105 -0.3Ni/$Al_2O_3$with brazing time variation (a) Brazing time 180s; (b) Brazing time 240s (c) Brazing time 300s;(d) Brazing time

Rare Metal Materials and Engineering
Rare Metal Materials and Engineering
Rare Metal Materials and Engineering

Fig.11 shows the microstructure of the interface IMC of the SAC105-0.3Ni/Al_2O_3 composite brazing joint. It can be seen from the figure that when the brazing time was 180s, the interface IMC was scallop shaped, with a relatively uniform particle size distribution and an average thickness of about 3.16um; When the brazing time was 240s, the overall interface IMC still presented a scallop like shape, with uneven particle sizes and an average thickness of about 3.27um; When the brazing time was 300s, the interface IMC showed a partially serrated shape, with uneven particle sizes and an average thickness of 3.34um; When the brazing time was 360s, the interface IMC transformed into a coarse serrated shape, with an average thickness of 4.32um.

During the brazing process, the growth of the interface IMC layer is a complex process. When Cu atoms and Sn atoms react

with each other to form Cu_6Sn_5 compounds, the further growth of interface IMC is mainly controlled by diffusion, including two stages: the first stage is grain boundary diffusion, and the second stage is bulk diffusion; The relationship between the thickness of IMC at the composite brazing interface and brazing time is shown in formula 1:

$$x=kt^n \quad (1)$$

Among them, x is the average thickness of interface IMC at different brazing times, and K is a constant; T is the brazing time; N is the time index of interface IMC growth

Take the logarithm of both sides of equation (1) to obtain equation (2)

$$\ln x=\ln k+n\ln t \quad (2)$$

Using lnt as the horizontal axis and lnx as the vertical axis, a linear function can be obtained by fitting, and the slope of the function interface is the growth index n of IMC. According to the fitting, the growth index n of IMC at the brazing interface of Ni/Al_2O_3 reinforced Sn1.0Ag0.5Cu composite brazing material is 0.39. According to literature research[36], when the interface IMC growth is controlled by grain boundary diffusion, the growth time index n is 0.33; When the growth of interface IMC is controlled by bulk diffusion, the growth time index n is 0.50. Therefore, the growth of interface IMC during the brazing process is the result of the combined effect of grain boundary diffusion and bulk diffusion.

3 Conclusion

1) Nickel coated alumina reinforcement phase was prepared by dopamine polymerization reaction and hydrothermal method. After the process of coating nickel with nano Al_2O_3, the nickel layer formed was uniform and continuous.

2) When the amount of Ni/Al_2O_3 varied according to the mass fraction of 0.1%, 0.3%, and 0.5%, the conductivity of the brazing alloy material slightly decreased.The overall wettability of composite materials was improved compared to the matrix materials, and the wettability was the best when the mass fraction of 0.3%.

3) When the amount of Ni/Al_2O_3 varied according to the mass fraction of 0.1wt%, 0.3wt%, and 0.5wt%,the overall tensile strength and elongation of the composite material were improved compared to the matrix. When the mass fraction of Ni/Al_2O_3 reached 0.3%, the tensile strength and elongation reached the maximum. At this point, the toughness of the fracture also reached the maximum.

4)The growth index of IMC at the brazing interface of Sn1.0Ag0.5Cu -0.3Ni/Al_2O_3 was linearly fitted to n=0.39, indicating that the growth of IMC at the interface was the result of the combined effect of grain boundary diffusion and bulk diffusion.

Reference

1 B F Huo, AZh, J A et al. Materials & Design[J]. 2021,25:32-38.

2 Sharma, A Baek, B GJung, JPuet al. Materials & Design [J]. 2015,87: 370-379.

3 S Habib, A H Pickel, A Det al. Progress in materials science[J]. 2015, 67:95-160.

4 S HMannan,H RKotadia,P DHoweset al. Microelectronics Reliability [J]. 2014,12:25-32.

5 Y L Lin,W Wanget al.Microelectronics Reliability[J].2014,8:56-65.

6 J Wu,S Xue, B,J W Wanget al. Journal of Materials Science[J]. 2016, 27:1-35.

7 H Ma,J C Suet al. Journal of Materials Science[J]. 2009, 44: 1141-1158.

8 A AEl-Daly,AFawzy,S FMansour et al. Materials Science & Engineering A [J].578:62-71.

9 ZLi,H Tang, Y Guoet al. Journal of Alloys and Compounds [J]. 2019, 818:152893.

10 Jung, Do-Hyun,Sharmaet al. Journal of Alloys and Compounds[J]. 2018,743:300-313.

11 S Shareeda, M Nasir, M Zamriet al.Ceramics international [J]. 2019, 79:20-27.

12 Z H, Li,Y Tang,Q WGuoet al. Journal of Alloys andCompounds[J]. 2019, 789, 150-162.

13 B Y Wang,Y J Wu, W Wuet al.Journal of Materials Science[J]. 57, 17491-17502.

14 J Wu,S Xue,J Wanget al. Journal of Materials Science. Materials in Electronics [J]. 2018, 29: 7372-7387.

15 RShalaby,M Elzanaty Het al. Journal of Materials Science. Materials in Electronics[J]. 2020, 31:5907-5913.

16 A Yakymovych,Y levachuk, Vec P et al. Journal of Materials Science. Materials in Electronics [J]. 2016,5:70-78.

Rare Metal Materials and Engineering

17 S Tikale, K N Prabhu et al. Materials Science &EngineeringA. Structural Materials: Properties, Misrostructure and Processin [J]. 2020,3: 787.
18 S Tikale,Narayan Prabhu et al. Transactions of the Indian In stitute of Metals[J]. 2018, 5:71.
19 L Tsao,S Chang,YLee et al. Materials & Design [J]. 2010, 31:4831-4835.
20 Y Wang,G Wang,K Song et al. Journal of Alloys and Com pounds [J]. 2017,119:219-224.
21 SS Tikale, K NPrabhu et al. Journal of Materials Science. Materials in Electronics [J]. 2021,6:78-84.
22 J H Wang, S B Xue, Z P LV et al. Progress in materials science [J]. 2019,33: 13.
23 J Yang, L Xu, K Xu et al. Steel Research International [J]. 2015,5:619–625.
24 H E Jia. J Sun, J Choi et al.Friction [J]. 2023, 11: 441-459.
25 C L Zhang. Nanjing University of Aeronautics and Astronautics [D].2016.
26 L Zhang, JG Zhang,FG Liu et al. Rare Metal Materials and Engineering [J] .2013, 42: 1897.
27 Israelachvili, J N Chu et al. Journal of Colloid & Interface Science[J]. 1987,116: 77.
28 K Landry,N Eustathopoulo etal.Acta Materialia[J]. 1996,44:3923-3932.
29 Y Wang, Z Fang,N Ma et al. Journal of materials science [J]. 2017,28: 94-99.
30 Y Lai, X Hu, X Jiang et al. Journal of Materials Engineering and Performance [J]. 2018, 27:564-6576.
31 Z Yang, W Zhou, P Wu et al. Journal of Materials Engineering & Performance [J]. 2014, 590:295-300.
32 KZ Wang, L Meng et al. Journal of Alloys & Compounds [J]. 2019, 5:781.
33 AAEl-Daly.AFawzy et al. Materials Science & Engineering A[J].2013,578:62-71.
34 FX Che, EC Poh et al.Electronics Packaging Technology Conference [J].2007,530:713-718.
35 ZB Yang, Wen Zhou, P Wu et al. Journal of materials science [J].2014,590:295-300.
36 D Q Yu, L Wanget al. Journal of Alloys & Compounds [J]. 2008, 458:542-547.

镍涂层 Al_2O_3 增强低银 SnAgCu 复合钎料的制备及钎焊性能研究

王冰莹[1,2]，张柯柯[1]，范玉春[1]，吴金娜[1]，郭李梦[2]，王悔改[1]，王楠楠[1]

（1 河南科技大学，河南洛阳 471000）

（2 洛阳理工学院，河南洛阳，471023）

摘要：采用多巴胺聚合反应和水热法制备了镍包覆氧化铝增强相；使用传统铸造方法制备镍包覆氧化铝(Ni/Al_2O_3) 增强 Sn1.0Ag0.5Cu (SAC105) 复合材料合金；结果表明，镍涂层是连续的，但厚度不均匀。镍与氧化铝之间的界面是冶金结合的半相干界面关系；SAC105 焊料与基体的强度、韧性和润湿性得到了改善，而导电性并没有显著降低。通过综合分析确定了最佳掺杂量为 0.3wt%。复合材料合金的断裂模式从韧脆性混合断裂模式转变为纯韧性断裂模式。然后将制备的复合钎焊材料制成焊膏进行铜板搭接实验。当掺杂量为 0.3wt%时，达到最大剪切强度。复合钎焊材料钎焊接头界面处 IMC 的生长指数线性拟合为 n=0.39，表明钎焊接头界面处 IMC 生长为晶界扩散和体扩散共同作用的结果。

关键词：复合钎料；增强相；聚合法；水热法；界面

作者简介：王冰莹，女，1984 年生，博士，讲师，河南科技大学，河南洛阳 471000，电话：15036327761，E-mail: 353315856@qq.com